

QUANTITATIVE AND STRUCTURAL ANALYSIS OF KALABAGH IRON ORE BY PHYSICO-CHEMICAL METHODS WITH REFERENCE TO ITS BENEFICIATION

Part III.—X-ray Analysis of the Component Mineral Phases

MAZHAR MAHMOOD QURASHI, SADRUL HASAN RIZVI AND M. LATIF AHMAD

Central Laboratories, Pakistan Council of Scientific and Industrial Research, Karachi

Introduction

In the previous communications^{1,2} of this series, analytical data have been given for random samples as well as specially collected representative samples of iron ore from the Kutch Khurtop mining property in Kalabagh. The results obtained by the chemical and physical methods agreed to within less than 1%, and a synopsis of the more significant data is given in Table 1. The iron content was found to vary from 22.4% to 39.2% for the representative samples drawn out from the various parts of the ore body. With reference to these figures it is noteworthy that the hand-picked sample from the area of the ore field leased out to Mr. Abdul Karim has 54% iron content. The analyses also point to the presence of nearly 25% of ferrous carbonate, but do not give any indication of the various structural forms in which the rest of the iron occurs. Such a structural study has now been carried out, and is described below. It has confirmed the presence of FeCO_3 and has further resulted in establishing the occurrence in appreciable quantities of three other ferruginous phases, namely chamosite, limonite, and hematite, all of which have an important bearing on the plan of beneficiation of the ore and its smelting, which are to be discussed in Part IV of this series of communications.

X-ray Patterns of the Five Main Samples

The X-ray diffraction technique has been employed as the one most suited to such structural studies, and powder patterns of the five typical samples taken with an 11.4 cm. diameter camera using filtered chromium $K\alpha$ radiation are shown in Fig. 1. It is significant that the "mean" and the "middle" samples, both of which contain nearly 34% iron, have almost identical patterns, while those of the other three show striking differences. Also, the large number of lines in the patterns suggests the existence of several important component structures corresponding to different chemical compounds or minerals. For the identification of these minerals, we must make a comparison with corresponding patterns of known standards, so as ultimately to account for all the observed lines, which are given in Table 2 along with their estimated intensities.

The preliminary identification was done by comparing the d-values of the strongest lines of the patterns with those given in the A.S.T.M. X-ray Data Cards³ and also with those of a standard pattern of $\alpha\text{-Fe}_2\text{O}_3$. This comparison showed that some hematite ($\alpha\text{-Fe}_2\text{O}_3$) is present in all the samples whose patterns appear in Fig. 1. Three important pairs of lines characteristic of this mineral

TABLE I.—SYNOPSIS OF ANYALYSES OF IRON ORE SAMPLES FROM KUTCH KHURTOP MINING AREA.

	Poorest sample	Richest sample	Middle sample	Mean Dump sample	From A. Karim's property
Iron %	22.4	39.2	34.7	33.5	54
Al_2O_3 %	..	11.0	..	13.0	..
Total SiO_2 %	..	15.2	..	24.2	..
CaO %	2.3	3.5	..	1.1	..
CO_2 %	6	6	..	11	..
H_2O %	5	6	..	2	..

TABLE 2.—d-VALUES IN ANGSTROMS AND ESTIMATED INTENSITIES OF THE LINES DOWN TO 1.3 A.U. IN THE OBSERVED POWDER PATTERNS OF THE FIVE TYPICAL SAMPLES OF IRON ORE.

s=strong ; m=medium ; w=weak ; f=faint ; d=diffuse.

A. Karim's sample		Mean sample		Middle sample		Richest sample		Poorest sample	
*f	6.95	m	7.20	w	7.25			m	7.20
		s	6.98	s	6.90	s	7.0	m	7.00
						f	4.60	m	6.00
								f	4.40
*f	4.20	f	4.15	f	4.20	s	4.15	f	4.35
f	3.68	f	3.67	f	3.65			f	4.25
		m	3.58	w	3.60			w	3.63
		m	3.51	w	3.55	m	3.50	w	3.53
		f	3.33	w	3.32				
**f	3.05	f	3.09					m	3.14
*f	2.80	s	2.80	s	2.80	f	2.80		
s	2.70	s	2.69	m	2.69	m	2.70	s	2.70
								f	2.55
s	2.50	s	2.52	s	2.50	m	2.52	s	2.50
*w	2.45	w	2.44	w	2.45	m	2.45		
		w	2.35	w	2.34			s	2.33
						f	2.25		
w	2.20	f	2.19			f	2.18	m	2.20
		m	2.14	s	2.12	f	2.13		
		m	1.96	m	1.96				
m	1.83	w	1.84	w	1.83	f	1.82	s	1.86
								s	1.85
				f	1.78			f	1.76
*f	1.71 ₀	m	1.73 ₇	s.d	1.72 ₅	w.d	1.73 ₀		
s	1.69 ₀	w	1.71 ₅	m	1.68 ₅	w	1.68 ₀	s	1.68 ₅
		m	1.69 ₅					m	1.65 ₅
		f	1.63 ₅						
m	1.59 ₅	f	1.59 ₆					w	1.59 ₅
*f	1.55 ₅	s	1.56 ₀	s	1.55 ₅	m.d	1.56 ₀		
		w	1.53 ₅	f	1.52 ₀	w.d	1.52 ₀		
		w	1.52 ₃						
*f	1.51 ₅	w	1.50 ₆	f	1.50 ₅				
s	1.48 ₅	m	1.48 ₈	m	1.49 ₀	f.d	1.47 ₅	s	1.48 ₅
s	1.45 ₀	m	1.45 ₈	m	1.45 ₀	f.d	1.45 ₀	s	1.45 ₀
*f	1.42 ₅	w	1.43 ₅	w	1.42 ₅	f.d	1.43 ₀	w	1.43 ₅
								f	1.39 ₅
		f	1.38 ₀	f	1.38 ₀			w	1.38 ₅
		f	1.37 ₅	f	1.37 ₅				
f	1.35 ₀								
		f	1.32 ₅						
w	1.31 ₀	f	1.31 ₀					s	1.31 ₀

* This denotes lines not due to hematite in the pattern of the sample from Mr. A. Karim's lease. These are comparatively faint and agree with the strongest lines of siderite, limonite and chamosite.

** Possibly due to chalcopyrite.

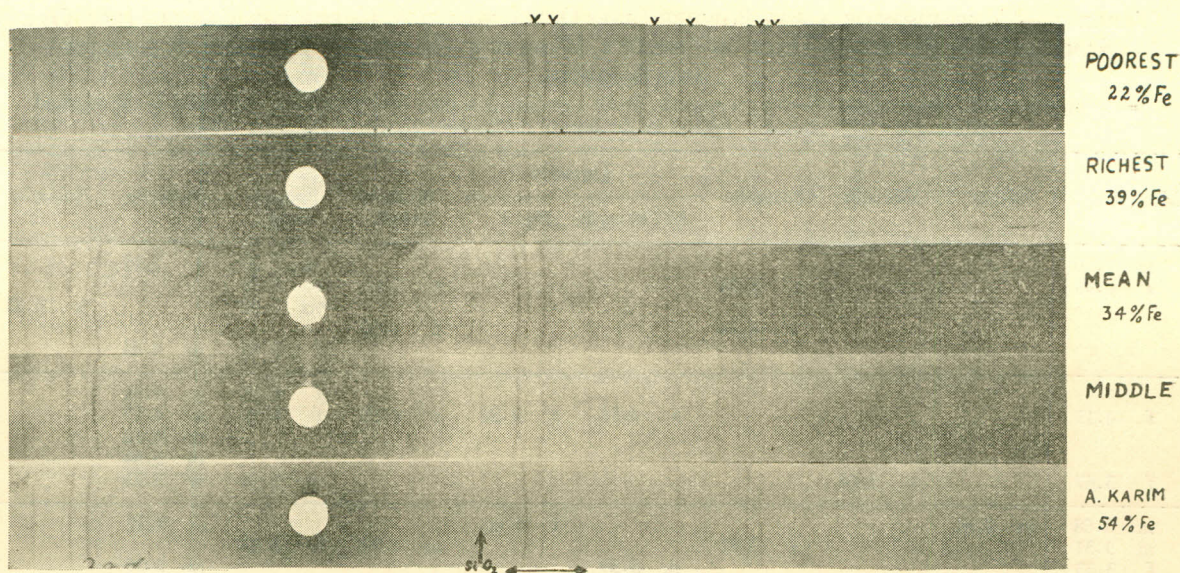


Fig. 1.—X-ray powder diffraction patterns of the five typical samples of Kalabagh iron ore, showing the complexity of the mean and middle samples; the only line due to quartz is marked SiO_2 with a vertical arrow (patterns taken with $\text{Cr K}\alpha$ filtered radiation). The region marked $\leftarrow\rightarrow$ shows strikingly the differences between the various patterns.

are marked with a "V" in the figure, and they can be seen in all the five patterns, although with different intensities. The pattern labelled "A. Karim" appears to be largely hematite because the intensities of all lines not due to hematite are very low in its pattern. This result is consistent with its high iron content (54%), because iron ores containing more than 50% iron consist mostly of the oxides of iron.

Identification of the Different Component Structures or Mineral Phases

(a) *Components of the Mean Sample.*—A search through the A.S.T.M. cards indicates that, in addition to hematite, the mean sample contains siderite (FeCO_3), chamosite (a ferruginous aluminosilicate usually containing 24 to 32% iron), and limonite ($\text{Fe}_2\text{O}_3 \cdot \text{H}_2\text{O} \cdot n\text{H}_2\text{O} = 2\text{FeO}(\text{OH}) \cdot n\text{H}_2\text{O}$). Confirmation of this is obtained by direct comparison with standard powder patterns as shown in Table 3 and Fig. 2, where the patterns of hematite ($\alpha\text{-Fe}_2\text{O}_3$), siderite and chamosite are placed alongside that of the mean representative sample, the resolved lines of chamosite being marked with arrows. It is seen that the siderite and hematite contributions to the pattern are of about equal intensity, thus indicating that the ore contains roughly equal quantities of the heavy atom (iron) in these two minerals. Taking their iron contents as 69% and 48% respectively, this gives a ratio of about 2:3 for hematite and siderite. About half a dozen lines remain outstanding after the siderite and hematite lines have been accounted

for, and most of these can be correlated with the stronger lines of chamosite, while the inner line of the strong low-angle doublet ($d=7.1 \text{ \AA}$) is probably due to kaolinite, two other lines of which appear somewhat indistinctly in our patterns. A weak spotty line (marked " SiO_2 " in Figs. 1 and 2) corresponding to the strongest quartz line is observed at 3.33 \AA . The contribution of the chamosite lines to the intensity of the whole pattern is also of the same order as that of siderite and hematite, whence we conclude (by an argument similar to the previous one) that these three minerals occur in the mean sample in the ratios of 2:3:4 approximately.

(b) *Components of the Richest Sample (39% Iron.)*—The X-ray patterns of the richest and poorest samples are both strikingly different from that of the mean sample in that the lines of siderite (FeCO_3) are absent, its strongest line at 2.80 \AA , (just inside the first strong doublet of $\alpha\text{-Fe}_2\text{O}_3$) being hardly detectable in the pattern of the richest sample (Fig. 1). Since the iron content is higher than the average, it follows that a large part of the iron must be present here in still another form, and the strong line just outside the first $\alpha\text{-Fe}_2\text{O}_3$ doublet appeared to belong to this new phase. After a thorough search, it was found that this phase is limonite ($\text{Fe}_2\text{O}_3 \cdot \text{H}_2\text{O} \cdot n\text{H}_2\text{O} = 2\text{FeO}(\text{OH}) \cdot n\text{H}_2\text{O}$), a somewhat diffuse pattern for which is shown alongside of the pattern of the richest sample in Fig. 3. This diffuse pattern of limonite was actually obtained when attempting

TABLE 3.—COMPARISON OF X-RAY POWDER LINES DOWN TO 1.3 Å. U. FOR THE VARIOUS IRON ORE SAMPLES WITH STANDARD DATA ON SIDERITE, HEMATITE, CHAMOSITE, LIMONITE, KAOLINITE AND BOHIMITE.

s=strong (50—100) ; m=medium (20—50) ; w=weak (10-20) ; f=faint (less than 10) ; d=diffuse ; faint lines in the standard pattern have been omitted. Almost all the lines of the limonite pattern in Fig. 3 are diffuse.

Mean sample	Siderite	Hematite	Chamosite	Limonite		Richest sample	Poorest sample	Kaolinite	Bohimitite
				ASTM cards	Fig. 3				
m 7.20 s 6.98			s 6.94 s 4.64			s 7.0 f 4.60	m 7.20 m 7.00 *m 6.00 f 4.40	s 7.15 m 4.45	s 6.11
f 4.15				s 4.18	s 4.20	s 4.15	f 4.35 f 4.25	s 4.35 s 4.17 m 4.12 m 3.84 w 3.73	
f 3.67		s 3.68					w 3.63		
m 3.58 m 3.51 f 3.33 f 3.09	m 3.61		s 3.51		f 3.60	m 3.50	w 3.53 *m 3.14	s 3.57 m 3.37 w 3.14 w 3.09	s 3.164
s 2.80 s 2.69 s 2.52 w 2.44	s 2.80	(f 2.79) s 2.69	m 2.78 w 2.69	s 2.69 m 2.58	s 2.69 f 2.59	f 2.80 m 2.70 m 2.52 m 2.45	s 2.70 f 2.55 s 2.50	w 2.75 s 2.55 m 2.52 s 2.486	
w 2.35	w 2.36						*s 2.33	s 2.374 s 2.331 s 2.284	s 2.346
f 2.19 m 2.14	w 2.13	s 2.20	m 2.13	s 2.19	m 2.20	f 2.25 f 2.18 f 2.13	m 2.20	m 2.182 w 2.127	
m 1.96	w 1.96							s 1.985 m 1.935	
w 1.84		s 1.837	m 1.77	w 1.83		f 1.82	*s 1.86 *s 1.85 f 1.76	w 1.892 m 1.825 s 1.778	m 1.860 m 1.850
m 1.737 w 1.715 m 1.695 f 1.635 f 1.596	m 1.73			s 1.72	m 1.725	w.d 1.730			
		s 1.691		w 1.69		w 1.680	s 1.685 m 1.655 w 1.595	s 1.659 s 1.616	w 1.662
s 1.560 w 1.535 w 1.523 w 1.506	w 1.50		s 1.56 m 1.53	s 1.56	m 1.570	m.d. 1.560		m 1.581 s 1.539	
					m 1.525	w.d. 1.520			
m 1.488 m 1.458 w 1.435		s 1.484 s 1.451	w 1.48			f.d. 1.475 f.d. 1.450	s 1.485 s 1.450 w 1.435	s 1.486	w 1.453
			w 1.43	w 1.42 w 1.40	m 1.425	f.d. 1.430	f 1.395		
f 1.380 f 1.375							w 1.385		
f 1.325 f 1.310		w 1.348 m 1.309		w 1.32			s 1.310		w 1.312

Note : The weak doublet given in parentheses in the hematite pattern is produced by the K β radiation (passing through the filter) and corresponds to the strong K α doublet at 2.6 ± 0.1 Å.

* Denotes lines in the pattern of the poorest sample that are accounted for by the bohimitite pattern only.

to take an X-ray powder pattern of FeCO_3 . It was found after several attempts that the carbonate invariably changed into the hydrated oxide, and the diffuseness of the lines in Fig. 3 is probably due to the incompleteness of the transformation. This phenomenon also suggests that the limonite in the richest sample may have resulted from deco-

mposition of siderite. The replacement of CO_2 by OH in the process would result in a loss of weight and therefore an increase in percentage iron content. The pattern of the richest sample is also remarkable for the fact that two comparatively weak lines of chamosite that overlap with other patterns in Fig. 2 are here clearly resolved,

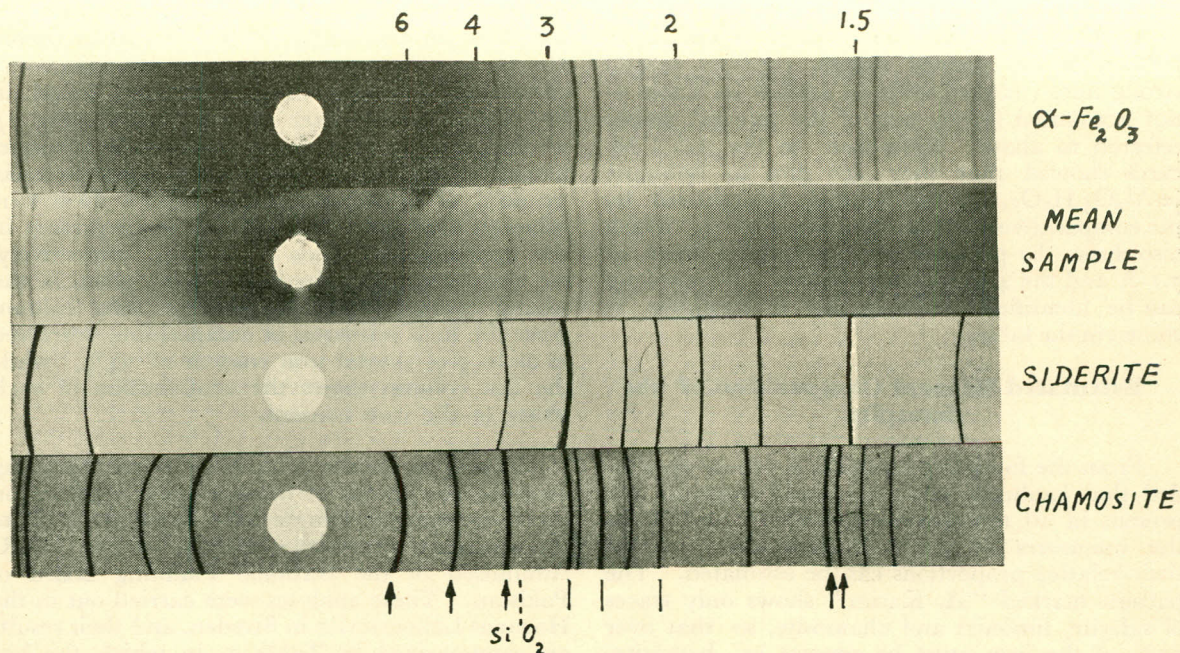


Fig. 2.—Comparison of the powder pattern of the mean sample with those of its constituent minerals, the arrows indicating the resolved lines due to chamosite. The patterns of siderite and chamosite have been made up from the standard data in the A.S.T.M. cards, the thicknesses of the lines being roughly proportional to the intensities. The scale at the top indicates d-values in Angstrom units.

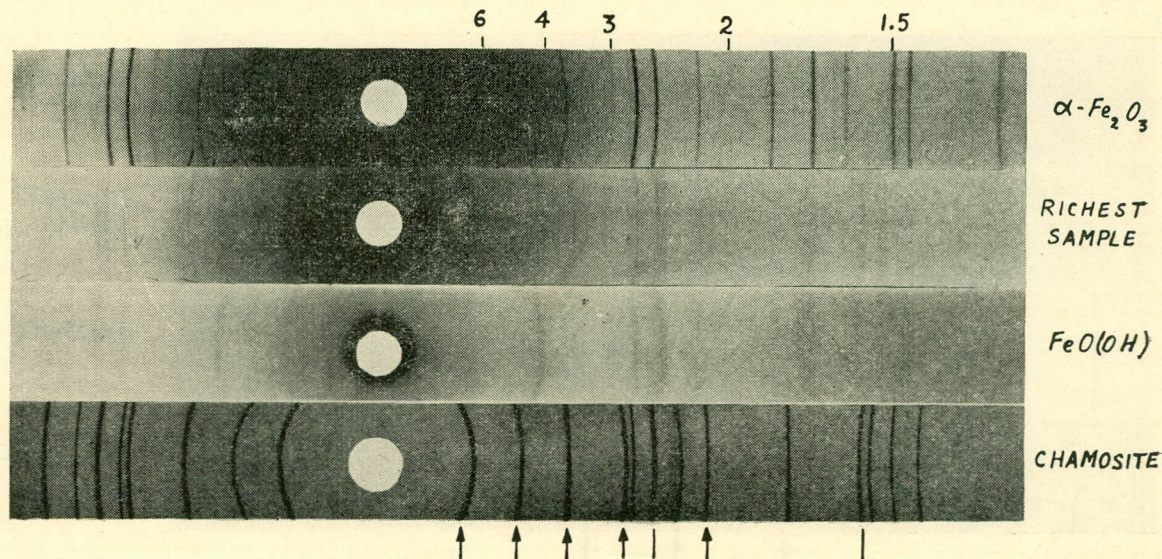


Fig. 3.—Comparison of the pattern of the richest sample with those of its constituent minerals, showing the replacement of siderite by limonite. The arrows indicate the resolved lines of chamosite. The scale at the top indicates d-values in Angstrom units.

as shown by the arrows in the 2-3 Å region. A detailed comparison of the lines of the patterns is given in Table 3, which moreover shows that the strongest lines of limonite are also to be found in the pattern of the mean sample, although with a very low intensity, corresponding to a limonite content of about half that of the hematite.

(c) *Components of the Poorest Sample.*—The X-ray pattern of the poorest sample contains several strong lines (marked with an asterisk in Table 3) not accounted for by any of the mineral phases referred to above. Reference to the A.S.T.M. cards showed that they are due to bohimite ($\alpha\text{-Al}_2\text{O}_3\cdot\text{H}_2\text{O}$), and this is clearly brought out by the comparative patterns shown in Fig. 4, which also shows the presence of unaccounted lines at 7.1 Å and the 4.3 Å group of lines. These lines can be identified as being due to kaolinite, as shown in the table.

Estimated Mineral Composition of the Samples

From the foregoing analysis, it can be concluded that kaolinite, chamosite, and hematite are present in all the samples examined, and from the intensities of their characteristic patterns, their relative proportions can be estimated. The pattern marked "A. Karim" shows only traces of siderite, limonite and chamosite, so that over 75% of the iron must be present as hematite. This type of ore would be excellent for treatment by a simple beneficiation and smelting process,

but it does not appear to be available in large quantities.

An accurate quantitative estimate of the kaolinite and bohimite in the mean sample is difficult to make from the X-ray data, and a figure of $10\% \pm 5\%$ is the best that can be obtained from the two or three weak lines available. If we allow another 10% for the free silica (noted above) and the traces of compounds of titanium, chromium, strontium and zirconium found in the X-ray spectrometer record (Part II, Fig. 1), we find that the ferruginous compounds, limonite, hematite, siderite, and chamosite, together make up 80% of the mean sample. Since these four minerals have been shown above to be present in the approximate ratios of 1:2:3:4, respectively, we immediately get the percentages given in the second column of Table 4. The next column gives the final estimates of composition, corrected so as to give a total iron content of 34%, while the last column shows the contribution of each phase to the iron content.

Subsequent to the completion of the foregoing analysis, the results of mineralogical analyses on the representative sample were made available to the authors through the courtesy of Mr. H. R. Amundsen of the National Planning Board of Pakistan. These analyses were carried out in the Hoganas Laboratories in Sweden, and their results are summarized in Table 5, in which the last column shows the estimated contributions of the various phases to the iron content. Comparison

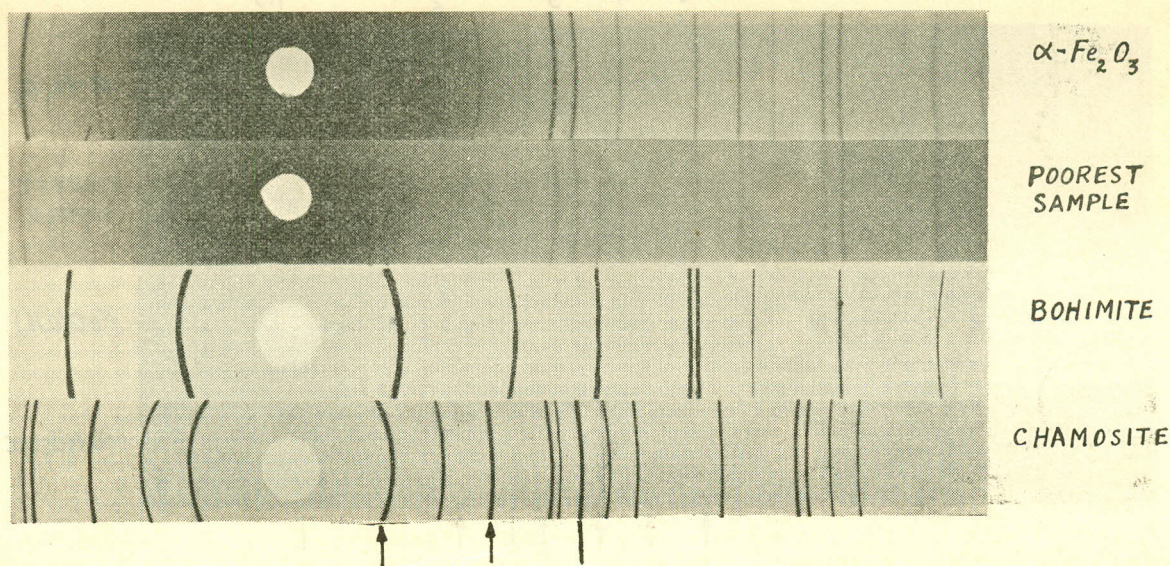


Fig.4.—Powder patterns showing the presence of bohimite, chamosite and hematite in the poorest sample. The pattern of bohimite (like that of chamosite) is made up from the standard data.

TABLE 4.—PERCENTAGE MINERAL COMPOSITION OF THE MEAN SAMPLE BY X-RAY ANALYSIS.

Constituent minerals	Weight % from X-ray analysis	Corrected values	Contribution to iron content
Limonite ($\text{Fe}_2\text{O}_3 \cdot \text{H}_2\text{O} \cdot n\text{H}_2\text{O}$)	8	7	4.5
Hematite ($\alpha\text{-Fe}_2\text{O}_3$)	16	14	9.8
Siderite (FeCO_3)	24	22	10.6
Chamosite* $3(\text{Fe, Mg})\text{O} \cdot \text{Al}_2\text{O}_3 \cdot 2\text{SiO}_2 \cdot n\text{H}_2\text{O}$..	32	30	8.4
$\text{TiO}_2, \text{Cr}_2\text{O}_3$ etc.	5	6	<1
Quartz	5	6	—
Kaolinite, bohimite	10 ± 5	15	—
Total	100	100	33.8 ± 0.5

* Chamosite is a ferruginous clay, and the formula given is therefore only approximate. It may contain 24-32% iron, and an average figure of 28% has been used in the table above.

of Tables 4 and 5 shows that in the main the results of the mineralogical analysis are in fair agreement with those of the X-ray analysis when allowance is made for the variability of the ore samples. However, there is a significant difference in that, on the basis of the analysis presented in this paper, a separate estimation of the limonite and the hematite can be made, whereas in Table 5 there is no reference to hematite, while the % given for the limonite indicates that both the hydrated and unhydrated forms of the oxide are included in that value. Another difference is that the aluminous sediments (corresponding to kaolinite and bohimite in Table 4) appear to have been underestimated in Table 5. These discrepancies are attributable partly to the difficulties inherent in the chemical method of analysis, and partly to the fact that for the present investigation several samples from different levels of the ore field were available, two of which (Figs. 3 and 4) were particularly rich in limonite and bohimite, respectively, thus facilitating their identification and estimation.

Decomposition of the Carbonate

When the siderite (FeCO_3) is completely decomposed (*e.g.*, by weathering) to give limonite [$\text{Fe}_2\text{O}_3 \cdot \text{H}_2\text{O} = 2\text{FeO}(\text{OH})$], there is a loss in weight of 24% on the weight of siderite. This should therefore raise the percentage weight of iron in the sample by a factor of $100 / (100 - 24 \times 0.24) =$

TABLE 5.—MINERALOGICAL ANALYSIS OF MEAN REPRESENTATIVE SAMPLE.

Constituent minerals	Analysis by Hoganas, Sweden	Contributions to iron content
Limonite ($\text{Fe}_2\text{O}_3 \cdot n\text{H}_2\text{O}$)	24.9	14.0 ± 2
Hematite (Fe_2O_3)
Siderite (FeCO_3) ..	25.6	12.3
Chamosite ..	35.6	9.0 ± 0.5
Ilmenite ($\text{FeO} \cdot \text{TiO}_2$) ..	1.7	0.6
Quartz ..	5.1	..
Residue (aluminous sediments)	7.7	..
Total ..	100.6	35.9 ± 2
Total iron by analysis =		35.8%

$100 / (100 - 6)$. The iron content calculated on this basis is 35.5%, thus only partly explaining the 39.2% of iron in the richest sample, which most probably also contains a higher percentage of the richest phase, hematite, than does the mean sample. In this connection it was of interest to study the decomposition of the carbonate by simple roasting at various temperatures. Fig. 5 shows comparative X-ray powder patterns of various portions of the mean sample heated for half an hour in an oven at three different temperatures, namely 450°C., 600°C. and 800°C.

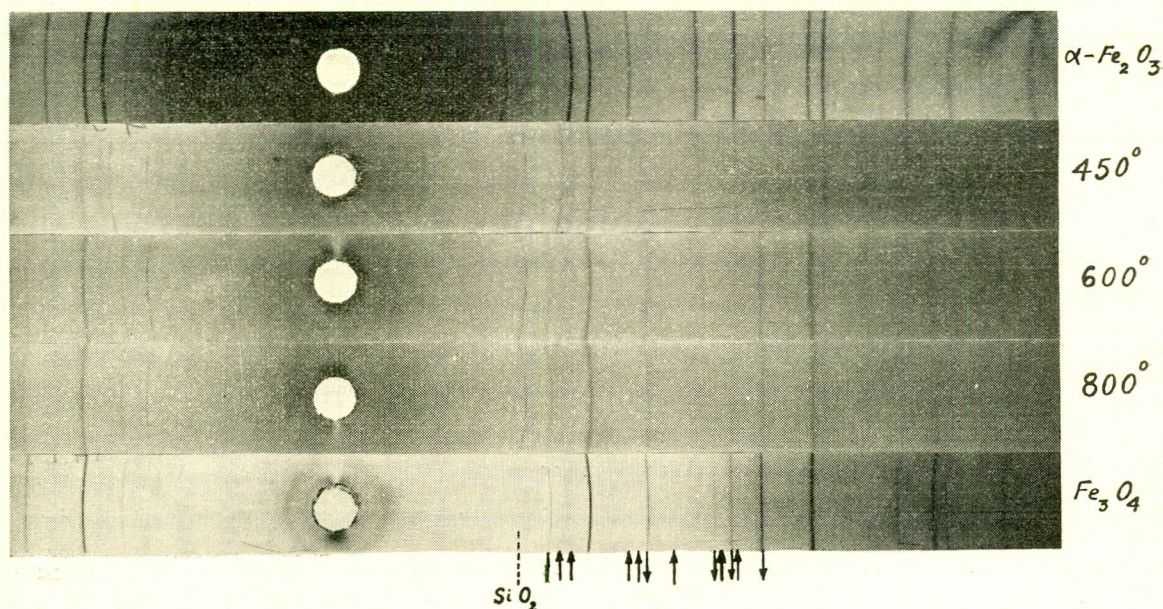


Fig. 5.—Powder patterns of roasted samples of ore compared with those of $\alpha\text{-Fe}_2\text{O}_3$ and Fe_3O_4 . The direction of the arrows indicate increasing intensity of the corresponding lines, and they show the progressive replacement of the hematite, limonite and siderite lines by those of Fe_3O_4 as the roasting temperature is raised (patterns taken with Cr K α filtered radiation).

The heat treatment at 450°C . has produced a barely detectable weakening of the siderite lines in the pattern, thus showing that very little of it is decomposed at this temperature. The patterns obtained after roasting at 600°C . and 800°C ., on the other hand, show the gradual disappearance of the lines of both siderite and hematite and their replacement by the lines of the magnetic oxide, Fe_3O_4 (and $\gamma\text{-Fe}_2\text{O}_3$), whose pattern is shown in the bottom of Fig. 5. Some typical lines that increase in intensity as we go from the top to the bottom are marked in the figure with arrows pointing downwards, while the disappearing lines of the initial phases are marked with arrows pointing upwards. A particularly interesting feature of Fig. 5 is that the pattern of chamosite also undergoes considerable modifications even at 600°C ., which suggests the desirability of further study of roasting as a likely means of beneficiation of this ore.

Conclusions

(a) The ore from the Kutch Khartop area contains about 50% of the iron oxides and ferrous carbonate, and more than 30% by weight of the ferruginous aluminosilicate, chamosite. The fine dissemination of the chamosite throughout the ore is likely to make its efficient beneficiation a complex process, unless hand-picking yields ore with a significantly lower chamosite content.

(b) Beneficiation by simple roasting or a modified roasting procedure presents an interesting possibility.

(c) Chemical treatment such as leaching etc. may have to be resorted to for the complete recovery of the iron from the ore. Since the ultimate choice of steel-making plant is likely to be governed by the economics of such beneficiation processes, their detailed study is in hand and the results will be reported in Part IV of this series of communications.

Acknowledgements

The authors are grateful to Dr. Salimuzzaman Siddiqui for his interest and encouragement, to Mr. Abdul Hai for helping with the experiments on the thermal decomposition of the ore, and to Mr. Howard Amundsen of the National Planning Board for making available the results of the mineralogical analyses of the ore.

References

1. S. H. Rizvi and M. M. Qurashi, Pakistan J. Sci. Ind. Research, **1**, 185 (1958).
2. H. R. Amundsen, A. Hashim, A. Hai and S. H. Rizvi, *ibid.*, **1**, 207 (1958).
3. American Society for Testing Materials: *X-ray Diffraction Data Cards* (1955).